01 Jan 2002

Experimental Verification of Derivatives Adaptive Critic Based Neurocontroller Performance on Single Turbogenerators on the Electric Power Grid

Ganesh K. Venayagamoorthy
Missouri University of Science and Technology

Donald C. Wunsch
Missouri University of Science and Technology, dwunsch@mst.edu

Ronald G. Harley

Recommended Citation

G. K. Venayagamoorthy et al., "Experimental Verification of Derivatives Adaptive Critic Based Neurocontroller Performance on Single Turbogenerators on the Electric Power Grid," *Proceedings of the 2002 International Joint Conference on Neural Networks, 2002. IJCNN '02*, Institute of Electrical and Electronics Engineers (IEEE), Jan 2002.
The definitive version is available at https://doi.org/10.1109/IJCNN.2002.1007792

Experimental Verification Of Derivatives Adaptive Critic Based Neurocontroller Performance On Single Turbogenerators On The Electric Power Grid

[1,3]G.K.Venayagamoorthy, *Member, IEEE*, [2]R.G.Harley, *Fellow, IEEE*, [3]D.C.Wunsch, *Senior Member, IEEE*
[1]School of Electrical and Electronic Engineering, University of Natal Durban 4041, South Africa.
[2]School of Electrical and Computer Engineering, Georgia Institute of Technology Atlanta GA 30332-0250 USA.
[3]Applied Computational Intelligence Laboratory, University of Missouri-Rolla, MO 65409-0249 USA.

Abstract – The design and real-time implementation of derivatives adaptive critic based neurocontrollers that replace the conventional automatic voltage regulators (AVRs) and turbine governors are presented in this paper. The feedback variables to the neurocontroller are completely based on local measurements from the turbogenerator. Experimental verification results are presented to show the superior performance of the derivatives adaptive critic based neurocontroller, compared to the conventional AVR and turbine governor controllers equipped with a power system stabilizer.

I. INTRODUCTION

Power systems containing turbogenerators are large-scale nonlinear systems. The traditional excitation controllers for the generators are designed by linear control theory based on a single-machine infinite bus (SMIB) power system model. These SMIB power system mathematical models are linearized at specific operating points and then excitation controllers are designed. The machine parameters change with loading in a complex manner, resulting in different behavior at different operating points and the controller which stabilizes the system under specific operating conditions, may no longer yield satisfactory results when there is a drastic change in the power system operating conditions and configurations. Conservative designs are therefore traditionally used, particularly in multimachine systems, to attempt satisfactory control over the entire operating range of the power system.

In recent years, renewed interest has been shown in power systems control using nonlinear control theory, particularly to improve system transient stability [1,2]. Instead of using an approximate linear model, as in the design of the conventional Power System Stabilizer (PSS), nonlinear models are used and nonlinear feedback linearization techniques are employed for the generator models, thereby alleviating the operating point dependent nature of the linear designs. Using nonlinear controllers, generator transient stability can be improved significantly. However, nonlinear controllers have a more complicated structure and are difficult to implement relative to linear controllers. In addition, feedback linearization methods require exact system parameters to cancel the inherent system nonlinearities, and this contributes further to the complexity of the stability analysis. However, the use of Artificial Neural Networks (ANNs) as neurocontrollers offers a possibility to overcome this problem.

Multilayer perceptron (MLP) type artificial neural networks are able to identify/model time varying single turbogenerator systems [3] and, with continually online training, these models can track the dynamics of the power system, thus yielding adaptive identification. ANN controllers have been successfully implemented on single turbogenerators using ANN identifiers and indirect feedback control [4,5]. Adaptive critics design have also been applied to control generators in a SMIB power system successfully in simulation [6,7] but no practical validation results have yet been presented.

The design and laboratory experimental evaluation of the performance of nonlinear neurocontrollers based on derivatives adaptive critic for a SMIB power system, to replace the traditional Automatic Voltage Regulators (AVRs) and turbine governors is discussed in this paper. The derivatives adaptive critic neurocontroller is based on the Dual Heuristic Programming (DHP) theory (a powerful member of the adaptive critics' family). With DHP, optimal neurocontrollers can be designed offline, avoiding the computational load of online learning and the issues of instability. The results show that both voltage regulation and system stability enhancement can be achieved with this proposed neurocontroller, regardless of the changes in the system operating conditions and configurations. This paper also shows that it is possible to have such neurocontrollers controlling turbogenerators in real time on the power grid.

II. SINGLE TURBOGENERATOR POWER SYSTEM

The practical laboratory power system [8] in Fig. 1 consists of a micro-alternator, driven by a dc motor whose torque - speed characteristics are controlled by a power electronic converter to act as a micro-turbine, and a single short transmission line which links the micro-alternator to an infinite bus.

The 3 kW, 220 V, three phase micro-alternator was designed to have all its per-unit parameters, except the field winding resistance, the same as those normally expected of a 1000 MW alternator. The micro-alternator parameters determined by the IEEE standards are given in Table 1 [8]. A time constant regulator is used to insert negative resistance in series with the field winding circuit, in order to reduce the actual field winding resistance to the correct per-unit value.
The conventional AVR and exciter combination transfer function block diagram is shown in Fig. 2 and the time constants are given in Table 2. The exciter saturation factor S_e is given by

0-7803-7278-6/02/$10.00 ©2002 IEEE

$$S_e = 0.6093\exp(0.2165V_{field}) \quad (1)$$

T_{v1}, T_{v2}, T_{v3} and T_{v4} are the time constants of the PID voltage regulator compensator; T_{v5} is the input filter time constant; T_e is the exciter time constant; K_{av} is the AVR gain; V_{fdm} is the exciter ceiling; and, V_{ma} and V_{mi} are the AVR maximum and minimum ceilings.

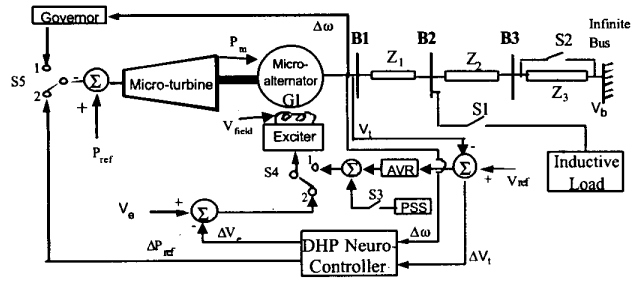

Fig. 1 Practical laboratory power system model (transmission line impedance $Z_1 = 0.01 + j0.25$, $Z_2 = 0.012 + j0.50$ and $Z_3 = 0.022 + j0.75$.

The micro-alternator is equipped with a PSS shown in Fig. 3. The PSS parameters are $T_w = 3$ s, $T_1 = 0.2$ s, $T_2 = 0.2$ s, $T_3 = 0.045$ s, $T_4 = 0.045$ s, $K_{STAB} = 33.93$, $Vpssmx = 0.2$ pu and $Vpssmin = -0.1$ pu.

TABLE 1
MICRO-ALTERNATOR PARAMETERS

$T_{d0}' = 6.69$ s	$T_{q0}'' = 0.25$ s	$X_d' = 0.205$ pu
$T_d' = 0.66$ s	$T_q'' = 27$ ms	$X_d'' = 0.164$ pu
$T_{d0}'' = 33$ ms	$T_{kd} = 38$ ms	$X_q = 1.98$ pu
$T_d'' = 26.4$ ms	$X_d = 2.09$ pu	$X_q'' = 0.213$ pu

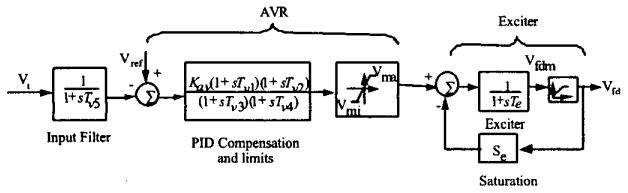

Fig. 2 Block diagram of the AVR and exciter combination.

TABLE 2
AVR AND EXCITER TIME CONSTANTS

T_{v1}	0.616 s	T_{v4}	0.039 s
T_{v2}	2.266 s	T_{v5}	0.0235 s
T_{v3}	0.189 s	T_e	0.47 s

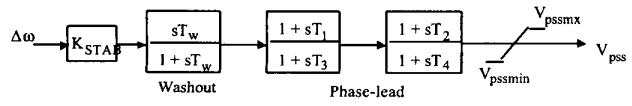

Fig. 3 Block diagram of the PSS.

A separately excited 5.6 kW dc motor is used as a prime mover, called the micro-turbine, to drive the micro-alternator. The torque-speed characteristic of the dc motor is controlled to follow a family of rectangular hyperbola for different positions of the steam valve, as would occur in a real typical high pressure (HP) turbine cylinder. The three low pressure (LP) cylinders' inertia are represented by appropriately scaled flywheels. The micro-turbine and the conventional governor transfer function block diagram is shown in Fig. 4, where, P_{ref} is the turbine input power set point value, P_m is the turbine output power, and ?? is the speed deviation. The turbine and governor time constants are given in Table 3.

Banks of lumped inductors and capacitors represent transmission lines of 1700 km, 400 kV. The practical system in Fig 1 is modeled in MATLAB/SIMULINK [5] to obtain simulated results for comparison with measured results.

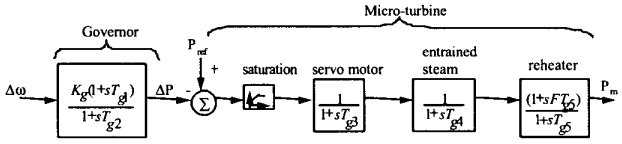

Fig. 4 Block diagram of the micro-turbine and governor combination.

TABLE 3
MICRO-TURBINE AND GOVERNOR TIME CONSTANTS

Phase advance compensation, T_{g1}	0.264
Phase advance compensation, T_{g2}	0.0264
Servo time constant, T_{g3}	0.15
Entrained steam delay, T_{g4}	0.594
Steam reheat time constant, T_{g5}	2.662
pu shaft output ahead of reheater, F	0.322

III. DERIVATIVE ADAPTIVE CRITICS' BASED NEURO-CONTROLLER

Adaptive Critic Designs (ACDs) are neural network designs capable of optimization over time under conditions of noise and uncertainty. A family of ACDs was proposed by Werbos [9] as a new optimization technique combining concepts of reinforcement learning and approximate dynamic programming. For a given series of control actions, that must be taken in sequence, and not knowing the quality of these actions until the end of the sequence, it is impossible to design an optimal controller using traditional supervised learning.

Dynamic programming prescribes a search which tracks backward from the final step, rejecting all suboptimal paths from any given point to the finish, but retains all other possible trajectories in memory until the starting point is reached. However, many paths which may be unimportant, are nevertheless also retained until the search is complete. The result is that the procedure is too computationally demanding for most real problems. In supervised learning, an ANN training algorithm utilizes a desired output and, comparing it to the actual output, generates an error term to allow learning. For

an MLP type ANN the backpropagation algorithm is typically used to get the necessary derivatives of the error term with respect to the training parameters and/or the inputs of the network. However, backpropagation can be linked to reinforcement learning via a network called the ***Critic*** network, which has certain desirable attributes.

Critic based methods remove the learning process one step from the control network (traditionally called the "***Action*** network" or "***actor***" in ACD literature), so the desired trajectory or control action information is not necessary [10]. The critic network learns to approximate the cost-to-go or strategic utility function, and uses the output of an action network as one of its inputs directly or indirectly. When the critic network learns, backpropagation of error signals is possible along its input pathway from the action network. To the backpropagation algorithm, this input pathway looks like just another synaptic connection that needs weight adjustment. Thus, no desired signal is needed. All that is required is a desired cost function J given in eq. (2).

$$J(t)=\sum_{k=0}^{\infty}\gamma^{k}U(t+k) \quad (2)$$

where γ is a discount factor for finite horizon problems ($0<\gamma<1$), and $U(.)$ is the utility function or local cost.

The Critic and the Action networks, can be connected together directly (Action-dependent designs) or through an identification model of a plant (Model-dependent designs). There are three classes of implementations of ACDs called Heuristic Dynamic Programming (HDP), Dual Heuristic Programming (DHP), and Globalized Dual Heuristic Dynamic Programming (GDHP), listed in order of increasing complexity and power [10]. This paper presents the DHP, model dependent design, and compares its performance against the results obtained using conventional PID controllers.

The critic network is trained forward in time, which is of great importance for real-time operation. DHP has a critic network which estimates the derivatives of J with respect to a vector of observables of the plant, ΔY. The critic network learns minimization of the following error measure over time:

$$\|E_C\|=\sum_{t}E_C^{T}(t)E_C(t) \quad (3)$$

where

$$E_C(t)=\frac{\partial J[\Delta Y(t)]}{\partial \Delta Y(t)}-\gamma\frac{\partial J[\Delta Y(t+1)]}{\partial \Delta Y(t)}-\frac{\partial U(t)}{\partial \Delta Y(t)} \quad (4)$$

where $\partial(.)/\partial\Delta Y(t))$ is a vector containing partial derivatives of the scalar (.) with respect to the components of the vector ΔY. The critic network's training is more complicated than in HDP since there is a need to take into account all relevant pathways of backpropagation as shown in Fig. 5, where the paths of derivatives and training of the critic are depicted by dashed lines.

In DHP, application of the chain rule for derivatives yields

$$\frac{\partial J(t+1)}{\partial \Delta Y_j(t)}=\sum_{i=1}^{n}\lambda_i(t+1)\frac{\partial \Delta Y_i(t+1)}{\partial \Delta Y_j(t)}+\sum_{k=1}^{m}\sum_{i=1}^{n}\lambda_i(t+1)\frac{\partial \Delta Y_i(t+1)}{\partial A_k(t)}\frac{\partial A_k(t)}{\partial \Delta Y_i(t)} \quad (5)$$

where $\lambda_i(t+1)=\partial J(t+1)/\partial\Delta Y_i(t+1))$, and n, m are the numbers of outputs of the model and the action networks, respectively. By exploiting eq. (5), each of n components of the vector $E(t)$ from eq. (4) is determined by

$$E_{Cj}(t)=\frac{\partial J(t)}{\partial \Delta Y_j(t)}-\gamma\frac{\partial J(t+1)}{\partial \Delta Y_j(t)}-\frac{\partial U(t)}{\partial \Delta Y_j(t)}-\sum_{k=1}^{m}\frac{\partial U(t)}{\partial A_k(t)}\frac{\partial A_k(t)}{\partial \Delta Y_j(t)} \quad (6)$$

The action network is adapted in Fig. 6 by propagating $\lambda(t+1)$ back through the model to the action.

The goal of such training can be expressed as:

$$\frac{\partial U(t)}{\partial A(t)}+\gamma\frac{\partial J(t+1)}{\partial A(t)}=0 \quad \forall t \quad (7)$$

The weights' update expression is:

$$\Delta W_A=-\alpha\left[\frac{\partial U(t)}{\partial A(t)}+\gamma\frac{\partial J(t+1)}{\partial A(t)}\right]^{T}\frac{\partial A(t)}{\partial W_A} \quad (8)$$

where α is a positive learning rate.

IV. THREE ARTIFICIAL NEURAL NETWORKS - MODEL, CRITIC AND ACTION

A DHP based neurocontroller is designed to replace the AVR and turbine governor on the micro-alternator G1 (Fig. 1); the ANN model of G1 (needed in Figs. 5 and 6) and the network to which it is connected, is obtained as described in [3]. The ANN MODEL in Figs. 5 and 6 is a three layer feedforward network with twelve inputs, a single hidden layer of fourteen neurons and two outputs. The inputs to the ANN are the *deviation* of the *actual* power ΔP to its turbine, the *deviation* of the *actual* exciter voltage ΔV_e to its exciter, the *deviation* of the *actual* speed $\Delta\omega$, and the *deviation* of the *actual* RMS terminal voltage ΔV_t of its micro-alternator, G1. These four inputs are also delayed by the sample period of 10 ms and, together with eight

previously delayed values, form twelve inputs altogether. For this set of inputs, the outputs are the *estimated* speed deviation $\Delta\hat{\omega}$ and the *estimated* terminal voltage deviation $\Delta\hat{V}_t$, of the micro-alternator, G1.

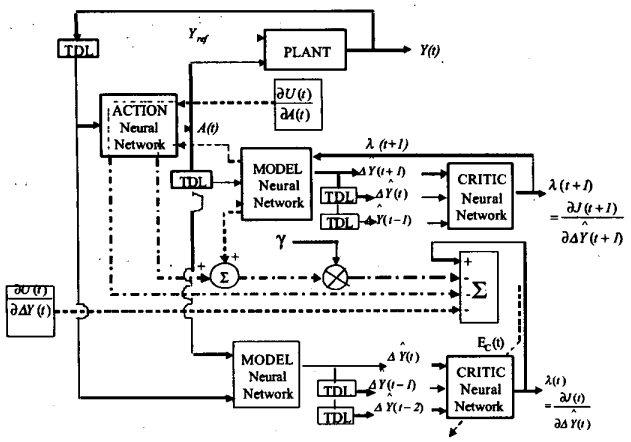

Fig. 5. DHP Critic network training.

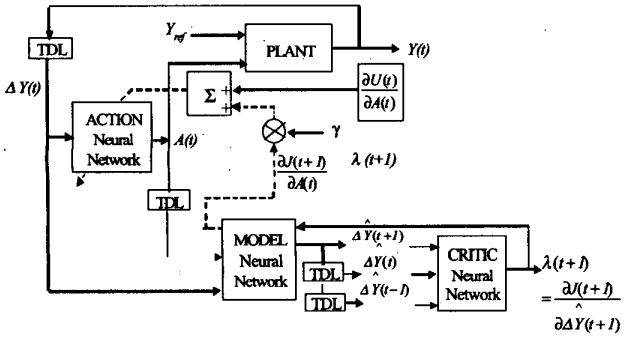

Fig. 6. DHP action network training.

The critic network in Figs. 5 and 6 is also a three layer feedforward network with six inputs, thirteen hidden neurons and, two outputs. The inputs to the critic network are the speed *deviation* $\Delta\omega$ and terminal voltage *deviation* ΔV_t. These inputs are time delayed by a sample period of 10 ms, and together with the four previously delayed values, form the six inputs for the critic network. The outputs of the critic are the derivatives of the J function with respect to the output states of the micro-alternator, G1.

The action network (DHP neurocontroller) in Figs. 5 and 6 is also a three layer feedforward network with six inputs, a single hidden layer with ten neurons and two outputs. The inputs are the micro-alternator's *actual* speed and *actual* terminal voltage deviations, $\Delta\omega$ and ΔV_t respectively. Each of these inputs is time delayed by 10 ms and, together with four previously delayed values, form the six inputs. The outputs of the action network (DHP neurocontroller), $A(t) = [\Delta V_e, \Delta P_{ref}]$, are the *deviation* in the exciter voltage, which augments the exciter voltage and the *deviation* in the turbine input power, which augments the input to the micro-alternator's turbine.

V. PRACTICAL IMPLEMENTATION OF THE DHP BASED NEURO- CONTROLLER

The practical implementation is carried out on the Innovative Integration M67 DSP card hosted by an IBM compatible PC with a Pentium III 433 MHz microprocessor. The M67 DSP card is based on the TMS320C67 160 MHz processor. The inputs to the exciter and micro-turbine, and the outputs of the micro-alternator are all sampled at 100 Hz using four A/D channels of the Innovative Integration A4D4 data acquisition card. The outputs of the A/D channels form the inputs to the neuroidentifier and neurocontroller. The outputs of the neurocontroller are passed through two D/A channels on the A4D4 card and added to the exciter and the turbine reference signals. One training cycle of either the DHP critic or action network is carried out in less than 4 ms. Once the DHP action network is trained, the real-time control on this M67 DSP card requires less than 1 ms of computation time for the forward propagation through the action network.

The practical training procedure for the critic and action networks are similar to those used in the simulation studies of adaptive critic designs for SMIB [6, 7]. It consists of two training cycles: the critic's and the action's. The critic's training is done initially with a pretrained action network, to ensure that the whole system, consisting of the ACD and the plant, remains stable. The action network is pretrained on a linearized model of the micro-alternator, G1. The action is trained further while keeping the critic network parameters fixed. This process of training the critic and the action one after the other is repeated until an acceptable convergence is achieved. The ANN model parameters are assumed to have converged globally during its offline training [3] and, it is not adapted concurrently with the critic and action networks.

A discount factor γ of 0.5 and the utility function given in eq. (8) are used in the Bellman's equation (eq. (1)) for the training of the critic network (eqs. (3)) and the action network (eq. (6)). Once the critic network's and action network's weights have converged, the action network (neurocontroller) is connected to the micro-alternator G1 (Fig. 1).

$$U(t) = [4\Delta V(t) + 4\Delta V(t-1) + 16\Delta V(t-2)]^2 + [0.4\Delta\omega(t) + 0.4\Delta\omega(t-1) + 0.16\Delta\omega(t-2)]^2 \quad (8)$$

VI. PRACTICAL RESULTS

At two different operating conditions and two different disturbances, the transient performance of the DHP neurocontroller is compared, with that of the conventional controllers (AVR and turbine governor) [11], as well as with that of the AVR equipped with a PSS (whose parameters are carefully tuned [12] for the first set of operating conditions).

A. An inductive load addition at the first operating condition (P = 0.2 pu, Q = 0 pu)

At the *first* operating condition, an inductive load , P = 0.8 pu at power factor (pf) of 0.85, is added to the transmission line at bus B2 by closing switch S1 (Fig. 1) at time t = 10 seconds. Figs. 7 and 8 show that the DHP neurocontroller ensures minimal overshoot on the terminal voltage as well as on the load angle unlike with the conventional controllers and even with AVR equipped with a PSS, and that the DHP controller also provides superior damping. The PSS improves the performance of the conventional controllers but still the DHP controller performs better. This is to be expected since the AVR and the PSS parameters have been tuned for only small disturbances at this operating point.

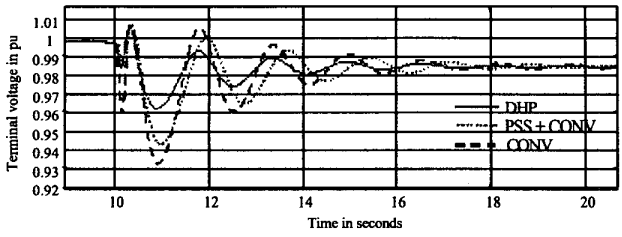

Fig. 7. Terminal voltage response for an inductive load addition at bus B2 (Fig. 1) for P = 0.2 pu & Q = 0 pu.

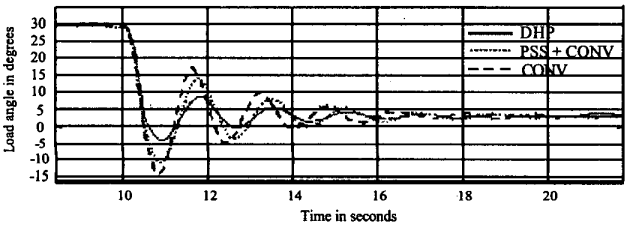

Fig. 8. Load angle response for an inductive load addition at bus B2 (Fig. 1) for P = 0.2 pu & Q = 0 pu.

B. Removal of a series transmission line at the first operating condition (P = 0.2 pu, Q = 0 pu)

At the *first* operating condition, the series transmission line impedance is decreased at time t = 10 seconds from Z = 0.0044 + j1.50 pu to Z = 0.0022 + j0.75 pu by closing switch S2 (Fig. 1). Figs. 9 and 10 show the terminal voltage and the rotor angle response for this test. Clearly that DHP neurocontroller again exhibits superior damping over the performance of the conventional controllers even when equipped with a PSS.

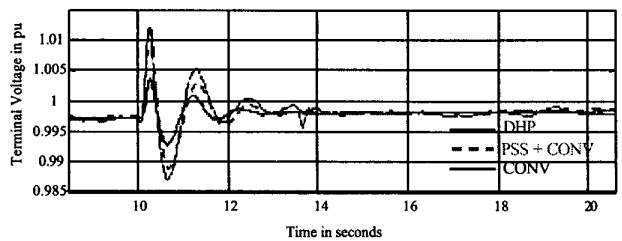

Fig. 9. Terminal voltage response for series transmission line impedance decrease by closing switch S2 (Fig. 1) for P = 0.2 pu & Q = 0 pu.

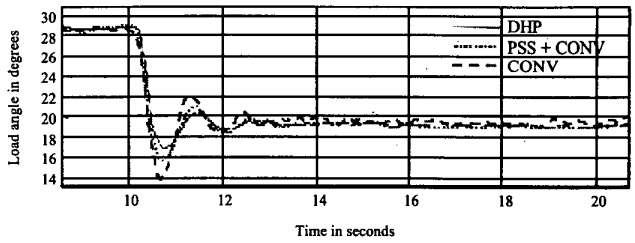

Fig. 10. Load angle response for series transmission line impedance decrease by closing switch S2 (Fig. 1) for P = 0.2 pu & Q = 0 pu.

C. An inductive load addition at the second operating condition (P = 0.3 pu, Q = 0 pu)

At the *second* operating condition, where the conventional controllers and PSS are not fine tuned to give their best performance, an inductive load , P = 0.8 pu at power factor (pf) of 0.85, is added to the transmission line at bus B2 by closing switch S1 (Fig. 1) at time t = 10 seconds. Figs. 11 and 12 show that the DHP neurocontroller again provides the best damping despite the change in the operating condition, unlike with the conventional controllers (AVR, governor and PSS). This proves that the DHP controller has learned the new operating condition and has the ability to perform robustly at all operating conditions. The damping of the DHP neurocontroller is far superior to the conventional controllers in both the terminal voltage and the load angle responses.

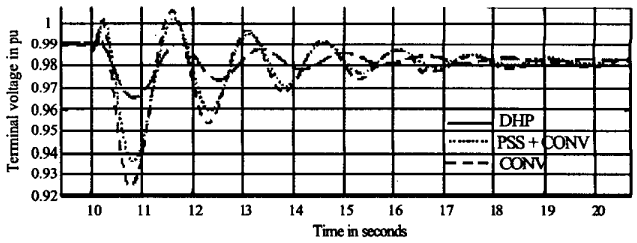

Fig. 11. Terminal voltage response for an inductive load addition at bus B2 (Fig. 1) for P = 0.3 pu & Q = 0 pu.

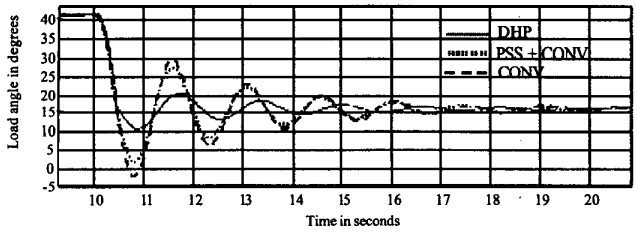

Fig. 12. Load angle response for an inductive load addition at bus B2 (Fig. 1) for P = 0.3 pu & Q = 0 pu.

D. Removal of a series transmission line at the second operating condition (P = 0.3 pu, Q = 0 pu)

At the *second* operating condition, the series transmission line impedance is increased at time t = 10 seconds from Z = 0.0044 + j1.50 pu to Z = 0.0022 + j0.75 pu by closing switch S2 (Fig. 1). Figs. 13 and 14 show the terminal voltage and the rotor angle response for this test.

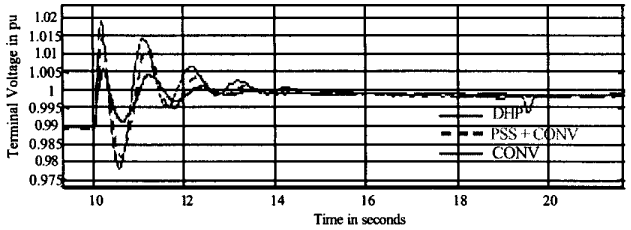

Fig. 13. Terminal voltage response for series transmission line impedance decrease by closing switch S2 (Fig. 1) for P = 0.3 pu & Q = 0 pu.

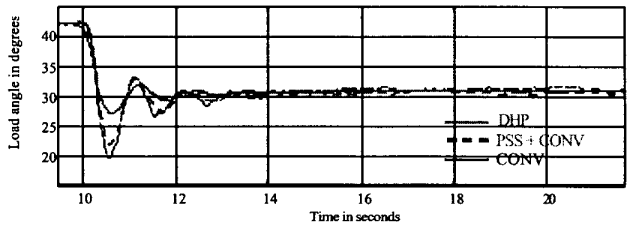

Fig. 14. Load angle response for series transmission line impedance decrease by closing switch S2 (Fig. 1) for P = 0.3 pu & Q = 0 pu.

Clearly that DHP neurocontroller again exhibits superior damping over the performance of the conventional controllers even when equipped with a PSS. Again, Figs. 13 and 14 show that the DHP neurocontroller provides the best damping despite the change in the operating condition, unlike with the conventional controllers (AVR, governor and PSS). This proves that the DHP neurocontroller has learned the new operating condition and has the ability to perform robustly at all operating conditions.

VII. CONCLUSIONS

These experimental studies on the practical implementation of an adaptive critic based neurocontroller to replace the conventional controllers are the first ones ever to show that a DHP neurocontroller can control a turbogenerator in real time. Experimental performance of such a neurocontroller has been evaluated against a conventional automatic voltage regulator equipped with a power system stabilizer and a turbine governor. The DHP neurocontroller exhibits superior robust damping at different operating points under different transient disturbances compared to the conventional controllers. This will allow generators equipped with DHP neurocontrollers to operate much closer to their steady state stability limits and still be able to remain transiently stable after severe disturbances and changes to the power system network. The next phase in this work is to extend the measurements to a system containing more than only one generator.

VIII. REFERENCES

[1] Q.Lu and Y.Sun, "Nonlinear Stabilizing Control of Multimachine Systems," *IEEE Trans. Power System*, vol. 4, pp. 236-241, 1989.

[2] J.W.Chapman, M.D.Ilic, C.A.King, L.Eng and H.Kaufman, "Stabilizing a Multimachine Power System via Decentralized Feedback Linearizing Excitation Control", *IEEE Trans. Powers System*, vol. 8, pp. 830-839, 1993.

[3] G.K.Venayagamoorthy and R.G.Harley, "Implementation of an Adaptive Neural Network Identifier for Effective Control of Turbogenerators", in *Proceedings of IEEE Power Tech Conference*, 1999, BPT99-431-6.

[4] G.K.Venayagamoorthy and R.G.Harley, "A Continually Online Trained Neurocontroller for Excitation and Turbine Control of a Turbogenerator", *IEEE Trans. on Energy Conversion*, vol. 16, no. 3, pp. 261-269, September 2001.

[5] G.K.Venayagamoorthy, R.G.Harley, "Simulation Studies with a Continuously Online Trained Artificial Neural Network Controller for a Micro-Turbogenerator", *in Proceedings of IEE International Conference on Simulation*, vol. 457, 1998, pp 405 – 412.

[6] G.K.Venayagamoorthy, D.C.Wunsch and R.G.Harley, "Neurocontrol of Turbogenerators with Adaptive Critics Designs", *in Proceedings of the IEEE Africon Conference*, vol. 1, 1999, pp. 489-494.

[7] G.K.Venayagamoorthy, R.G.Harley, and D.C.Wunsch, "Comparison of a Heuristic Dynamic Programming and a Dual Heuristic Programming based Adaptive Critics Neurocontroller for a Turbogenerator", in *Proceedings of the International Joint Conference on Neural Networks*, IJCNN 2000, pp. 233 – 238.

[8] D.J.Limebeer, R.G.Harley and S.M.Schuck, "Subsychronous Resonance of Koeberg Turbogenerators and of a Laboratory Micro-alternator System", *Transactions of the South African Institute of Electrical Engineers*, pp. 278-297, November 1979.

[9] P.Werbos, "Approximate Dynamic Programming for Real-Time Control and Neural Modeling, in *Handbook of Intelligent Control*, White and Sofge, Eds., Van Nostrand Reinhold, ISBN 0-442-30857-4, pp 493 – 525.

[10] D.Prokhorov, D Wunsch, "Adaptive Critic Designs", *IEEE Trans. on Neural Networks*, vol. 8, no.5, pp 997-1007, 1997.

[11] W.K.Ho, C.C.Hang, L.S.Cao, "Tuning of PID Controllers based on Gain and Phase Margin Specifications", in *Proceedings of the 12th Triennial World Congress on Automatic Control*, 1993, pp. 199 –202.

[12] P.Kundur, M.Klein, G.J.Rogers, M.S.Zywno, "Application of Power System Stabilizers for Enhancement of Overall System Stability ", *IEEE Trans. on Power Systems*, vol. 4, no. 2, pp. 614-626, May 1989.